IL NUOVO CIMENTO **47 C** (2024) 215
DOI 10.1393/ncc/i2024-24215-8

COLLOQUIA: HADRON2023

Electroweak structure of the nucleon

F. ALVARADO(1)(*), A. DI(2)(**), L. ALVAREZ-RUSO(1)(***) and S. LEUPOLD(2)(**)

(1) *Instituto de Física Corpuscular (IFIC) and Departamento de Física Teórica, Consejo Superior de Investigaciones Científicas (CSIC) and Universidad de Valencia (UV) E-46980 Paterna, Valencia, Spain*

(2) *Institutionen för fysik och astronomi, Uppsala universitet - Box 516, S-75120 Uppsala, Sweden*

received 21 December 2023

Summary. — The nucleon form factors (FFs) are studied in relativistic chiral perturbation theory (ChPT) in two flavors with explicit $\Delta(1232)$ degrees of freedom. For the electromagnetic isovector form factors we also employ dispersion theory to account for ρ-dominated isovector $\pi\pi$ interaction and its quark-mass dependence in the t-channel nonperturbatively and beyond NLO in ChPT. With this framework we explore how LQCD data are described in both the Q^2 and M_π dimensions simultaneously. Furthermore, we have performed an NNLO calculation of the nucleon axial form factor, extracting relevant low-energy constants (LECs) from a combined set of recent LQCD results from different collaborations.

1. – Electroweak form factors in ChPT

Nucleon electroweak FFs contain relevant details about hadronic structure and strong interactions in the nonperturbative regime. This information is encoded in their dependence on the momentum transferred to the nucleon by external probes but also in their quark-mass dependence, which is accessible by LQCD simulations. We calculate the nucleon isovector electromagnetic and axial form factors in ChPT, modifying the first one with dispersive relations.

(*) E-mail: Fernando.Alvarado@ific.uv.es
(**) E-mail: di.an@physics.uu.se
(***) E-mail: Luis.Alvarez@ific.uv.es
(**) E-mail: stefan.leupold@physics.uu.se

2. – Electromagnetic form factors

The electromagnetic FF receives a substantial resonance contribution, from the ρ meson, which motivates our use of dispersive relations. The dispersive relation at low energies is approximately

$$F(q^2) \approx \int_{4M_\pi^2}^{\Lambda^2} \frac{\mathrm{d}s}{\pi} \frac{\mathrm{Im}F_{2\pi}(s)}{s - q^2 - i\epsilon} + F_{\text{ChPT without } 2\pi\text{cut}}(q^2). \tag{1}$$

The first term on the rhs is the dispersive treatment for those diagrams where the photon couples to two pions. The second term stays for the rest of diagrams, that we include up to one loop in ChPT.

In the dispersive calculation, we employ the IAM method to obtain the phase shift and its M_π dependence, that we check with the LQCD results of [1]. Following (1), we combine the dispersive calculation with relativistic ChPT with extended on mass shell renormalization and explicit Δ. The details of the dispersive and the ChPT calculations can be found in [2]. We then fit the unknown LECs to the LQCD data of [3] and analyze the results.

2˙1. *Dirac form factor.* – For the Dirac FF we include ChPT diagrams up to $\mathcal{O}(p^3)$ and the only free parameter in the combined dispersive and ChPT description is d_6. We observe that the fit is good for $Q^2 < 0.6\,\mathrm{GeV}^2$ and all the M_π, *i.e.*, $M_\pi \leq 350\,\mathrm{MeV}$. In fig. 1 (left) one can see the curve of the combined description, compared with pure dispersive and plain ChPT ones (details in [2]). The combined curve is a better description than the other two, yielding a smaller χ^2 as shown in table I. On top of that, the combined description does not deviate too much from the experimental Kelly parametrization.

Turning to the radius and the M_π dependence, the combined description yields a better χ^2 behaviour with respect to M_π than ChPT. At the physical point, we extract $\langle r_1^2\rangle_{\text{phys}}^{\text{disp+ChPT}} = 0.4838 \pm 0.0047\,\mathrm{fm}^2$, in tension with the experimental value. This may

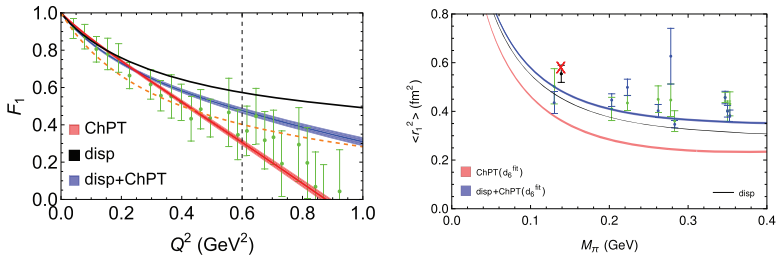

Fig. 1. – Left: $F_1(Q^2)$ at the physical point for the three descriptions. Black, red, and blue bands stay for the pure dispersive prediction, plain ChPT and the combined calculation. The bands show the 1σ statistical error. The dashed orange curve is the Kelly parametrization of the experimental F_1 ref. [4]. The points are the LQCD physical ensemble. Right: $\langle r_1^2\rangle(M_\pi)$ curves. The points are the LQCD extraction from [3] using the z-expansion to parametrize the Q^2 dependence of F_1 (green and blue correspond to summation and two-particle method, respectively). The black point is an extraction of ref. [3] and the red one is the experimental one [5].

TABLE I. – *Results of the* $F_1(Q^2, M_\pi)$ *and* $F_2(Q^2, M_\pi)$ *fits to LQCD in the top and bottom tables, respectively. The experimental values are* $\langle r_1^2\rangle_{\rm phys} = 0.577 \pm 0.0018\, fm^2$, $\kappa = 3.706$ *and* $\langle r_2^2\rangle = 0.7754 \pm 0.0080\, fm^2$ *(PDG* [5]*).*

F_1	disp	ChPT	disp+ChPT	HB from [3]
χ^2/dof	2.32	1.61	0.53	
$\langle r_1^2\rangle_{\rm phys}$ (fm^2)	0.4541	0.3626 ± 0.0047	0.4838 ± 0.0047	0.554 ± 0.035
F_2	disp	ChPT	disp+ChPT	HB from [3]
χ^2/dof	1.11	1.03	1.30	
$\kappa_{\rm phys}$	3.632 ± 0.037	3.423 ± 0.059	3.605 ± 0.067	3.71 ± 0.17
$\langle r_2^2\rangle_{\rm phys}$ (fm^2)	0.792 ± 0.011	0.61885 ± 0.0069	0.788 ± 0.015	0.690 ± 0.042

be a consequence of the fact that we are not estimating a theoretical uncertainty or it could be due to some missing LQCD systematics.

2˙2. *Pauli form factor.* – We follow an analogous procedure with the Pauli FF. The main difference is that F_2 starts at higher order in ChPT, so that we include the $\mathcal{O}(p^4)$ $\not\Delta$ in the ChPT term. This leads to three LECs that we fit to the same LQCD study [3] in the same range as for F_1 (details in [2]). In this case, the plain ChPT and the pure dispersive theories on their own perform well enough to describe the data. One can see the results in figs. 2, 3 and table I. In particular, the pure dispersive and the combined descriptions agree closely with the experimental parametrization above the fit limit $Q^2 = 0.6\,\text{GeV}^2$.

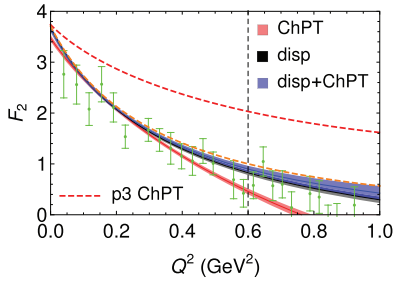

Fig. 2. – $F_2(Q^2)$ at the physical point for the three schemes (same colors as in fig. 1).

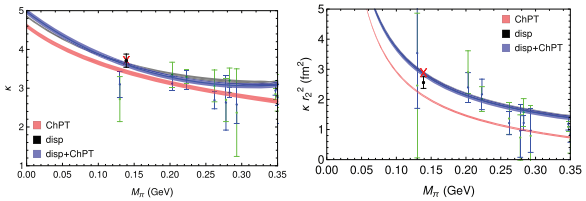

Fig. 3. – κ (left panel) and $\kappa\langle r_2^2\rangle \sim F_2'(0)$ (right panel) *vs.* M_π for the three schemes together with LQCD and experimental points (same colors as in fig. 1).

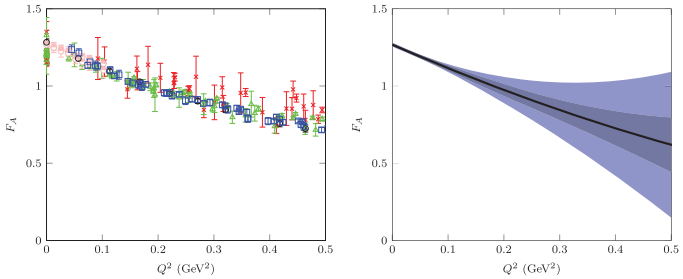

Fig. 4. – Left: the points are the lattice $F_A(Q^2)$ at different M_π. Red, green, pink, black and blue points belong to "Mainz" [6], RQCD [7], PACS [8], ETMC [9] and NME [10], respectively. Right: our $F_A(Q^2)$ fit at the physical point. The dark band shows the 1σ statistical errors. The light band corresponds to the theoretical uncertainty.

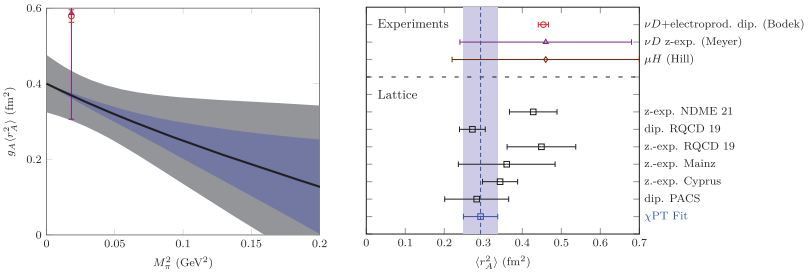

Fig. 5. – Left: $g_A\langle r_A^2\rangle$ *vs.* M_π^2. Right: comparison of our $\langle r_A^2\rangle$ with other determinations. (Bodek), (Meyer) and (Hill) correspond to [11], [12] and [13], respectively.

Finally, $\kappa_{\text{phys}}^{\text{disp+ChPT}} = 3.605 \pm 0.067$ are extracted from the combined model, and $\langle r_2^2\rangle_{\text{phys}}^{\text{disp+ChPT}} = 0.788 \pm 0.015\,\text{fm}^2$, close to the experimental values in table I.

3. – Axial form factor

Turning to the other term of the electroweak interaction, we calculate now the isovector axial form factor, F_A, as defined in [14]. It provides information on the spin distribution within the nucleon and is a key ingredient of neutrino cross sections. This form factor is a much more challenging quantity than the electromagnetic one from the experimental side. In fact, a large effort has been made by the LQCD community in order to shed light on this quantity. Notably, the LQCD results have improved in the recent years, in particular in the reduction of the systematic error.

In general, any analysis of the axial form factor and extraction of its radius is strongly dependent on the Q^2 (and M_π for LQCD) parametrization employed. In this respect, ChPT provides a parametrization in both variables given by the symmetries of QCD. This is the motivation of our work: we calculate F_A up to $\mathcal{O}(p^4)$ in relativistic ChPT with explicit Δ and fit the unknown LECs to a combined set of LQCD results. Therefore we obtain an axial FF which does not depend on a particular parametrization ansatz.

The LQCD data for the fit is taken from: RQCD [7], NME [10], "Mainz" [6], PACS [8] and ETMC [9] (fig. 4). We fit the seven free LECs (correcting for lattice spacing effects)

and implement the uncertainty of truncating the chiral series. We obtain a good description of the data for $Q^2 < 0.36\,\mathrm{GeV}^2$ and $M_\pi < 400\,\mathrm{MeV}$ (fig. 4 and fig. 5 for $\langle r_A^2\rangle(M_\pi)$). We extract $\langle r_A^2\rangle^{\mathrm{phys}} = 0.291 \pm 0.052\,\mathrm{fm}^2$ free of *ad hoc* parametrization (see [15] for g_A) which reflects the overall tension between the LQCD extractions and experimental (model-dependent) determinations.

* * *

This work has been supported by the Swedish Research Council (Vetenskapsrådet) (grant No. 2019-04303), the Spanish Ministerio de Ciencia e Innovación under contracts FIS2017-84038-C2-1-P and PID2020-112777GB-I00, the EU STRONG-2020 project under the program H2020-INFRAIA-2018-1, grant agreement No. 824093 and by Generalitat Valenciana under contract PROMETEO/2020/023.

REFERENCES

[1] Andersen Christian, Bulava John, Hörz Ben and Morningstar Colin, *Nucl. Phys. B*, **939** (2019) 145.
[2] Alvarado Fernando, An Di, Alvarez-Ruso Luis and Leupold Stefan, *Light quark mass dependence of nucleon electromagnetic form factors in dispersively modified chiral perturbation theory*, arXiv:2310.07796 (2023).
[3] Djukanovic D., Harris T., von Hippel G., Junnarkar P. M., Meyer H. B., Mohler D., Ottnad K., Schulz T., Wilhelm J. and Wittig H., *Phys. Rev. D*, **103** (2021) 094522.
[4] Kelly J. J., *Phys. Rev. C*, **70** (2004) 068202.
[5] Workman R. L. *et al.*, *PTEP*, **2022** (2022) 083C01.
[6] Capitani Stefano, Della Morte Michele, Djukanovic Dalibor, von Hippel Georg M., Hua Jiayu, Jäger Benjamin, Junnarkar Parikshit M., Meyer Harvey B., Rae Thomas D. and Wittig Hartmut, *Int. J. Mod. Phys. A*, **34** (2019) 1950009.
[7] Bali Gunnar S., Barca Lorenzo, Collins Sara, Gruber Michael, Löffler Marius, Schäfer Andreas, Söldner Wolfgang, Wein Philipp, Weishäupl Simon and Wurm Thomas, *JHEP*, **05** (2020) 126.
[8] Shintani Eigo, Ishikawa Ken-Ichi, Kuramashi Yoshinobu, Sasaki Shoichi and Yamazaki Takeshi, *Phys. Rev. D*, **99** (2019) 014510; **102** (2020) 019902(E).
[9] Alexandrou C. *et al.*, *Phys. Rev. D*, **103** (2021) 034509.
[10] Park Sungwoo, Gupta Rajan, Yoon Boram, Mondal Santanu, Bhattacharya Tanmoy, Jang Yong-Chull, Joó Bálint and Winter Frank, *Phys. Rev. D*, **105** (2022) 054505.
[11] Bodek A., Avvakumov S., Bradford R. and Budd Howard Scott, *Eur. Phys. J. C*, **53** (2008) 349.
[12] Meyer Aaron S., Betancourt Minerba, Gran Richard and Hill Richard J., *Phys. Rev. D*, **93** (2016) 113015.
[13] Hill Richard J., Kammel Peter, Marciano William J. and Sirlin Alberto, *Rep. Prog. Phys.*, **81** (2018) 096301.
[14] Yao De-Liang, Alvarez-Ruso Luis and Vicente-Vacas Manuel J., *Phys. Rev. D*, **96** (2017) 116022.
[15] Alvarado Fernando and Alvarez-Ruso Luis, *Phys. Rev. D*, **105** (2022) 074001.